An investigation into the hammer toe effects on the lower extremity mechanics and plantar fascia tension: A case for a vicious cycle and progressive damage.

Mohammad Moayedi
Amirkabir University of Technology
Ahmad Reza Arshi (arshi@aut.ac.ir)
Amirkabir University of Technology
Manouchehr Salehi
Amirkabir University of Technology
Mohammad Akrami
University of Exeter
Noushin Javadi Asl
Amirkabir University of Technology
Roozbeh Naemi
Staffordshire University

Article

Keywords: Plantar fascia, Hammer toe, Finite element analysis, Plantar soft tissue, Diabetic foot ulcer

Posted Date: June 17th, 2022

DOI: https://doi.org/10.21203/rs.3.rs-1758484/v1

Abstract

Predicting and being aware of the side effects of the damage in one limb on the performance of other limbs is very important in the prevention of progressive damages. Finite element (FE) and musculoskeletal modeling can be helpful in this way. Hence, the aim of this study is to investigate the side effects of the hammer toe deformity on the lower extremity, especially on the plantar fascia functions. To compare the joint reactions of the hammer toe and healthy foot (HF), two musculoskeletal models (MSM) of the healthy and the hammer toe foot (HTF) subject were developed based on gait analysis. A previously validated 3D finite element model was constructed using Magnetic Resonance Imaging (MRI) of the diabetic participant with the hammer toe deformity processed at five different events during the stance phase of gait.

It was found that the hammer toe deformity makes dorsiflexion of the toes, and the windlass mechanism is less effective during walking. Specifically, the FE analysis results showed that plantar fascia (PF) in HTF compared to HF played a less dominant role in load bearing with both medial and lateral parts loaded. Also, the results indicated that the stored elastic energy in PF was less in HTF than the HF, which can indicate a metabolic cost during walking. Internal stress distribution shows that the majority of ground reaction forces are transmitted through the lateral metatarsals in hammer toe foot, and the probability of fifth metatarsal fracture and also progressive deformity like tailor's bunion was subsequently increased. The MSM results showed that the joint reaction forces and moments in hammer toe foot have deviated from normal function, with the metatarsophalangeal joint showing that the reactions in hammer toe are less than the healthy foot. This can indicate a viscous cycle of foot deformity, increased internal stresses, change in muscle forces and joint kinetics and plantar fascia tensile forces from normal, which can lead to increase the risk of ulceration in the diabetic foot.

1. Introduction

The human body is a complicated mechanism with so many components that an operational issue in one section might impact the other and potentially cause the entire mechanism to deteriorate. Lower extremity health is a critical aspect of overall life quality that is influenced by various factors, including age, weight, musculoskeletal disorders, daily activities, and footwear [1–6]. Some of the techniques that can be used to obtain appropriate information about the various internal tissues and elements functions are musculoskeletal and finite element modeling[7–9], gait analysis [10, 11], and in-Vivo tests [12–15]. These techniques’ data cause better identification of biomechanical body parameters, especially in the lower extremity.

The health of the limbs has long been a priority and should be more accurate for diabetics to avoid injury, particularly on the foot area. Diabetic ulceration has been widely studied in previous researches [16–19], which shows that this issue is more important for diabetics. Excessive mechanical forces are one of the causes of foot ulcers [20, 21]. Foot deformities can change the force distribution in components of the foot such as the plantar and bones and also can be the starting point for progressive damage such as

foot ulcers [22–24]. Some injuries and damages in one area cause problems in another. Various studies have been conducted to see whether damage and deformity in one part of the foot might lead to harm in other sections of the body, such as the ankle, knee, and hip. The effect of flat feet [25–27], hallux [28, 29], and foot arch[30–32] on other portions of the lower limb are among them. The plantar fascia and joints are the significant elements of the locomotor organs. Forces and moments of the joints have been regarded in several types of researches as the factors that may be studied in joints [33–38].

PF function and pathologies were considered in previous studies [39, 40]. The plantar fascia is a thick band of connective tissue that crosses the bottom of the foot, extending from the calcaneus to the base of the toes. PF plays important roles in foot arch support, stress distribution (load-sharing), energy storage and shock absorption during walking [41]. As mentioned in several studies, plantar fascia stores elastic energy during the first half of the stance phase and some portion of this stored energy returns to the foot during the longitudinal arch recoiling at the late stance phase which brings a part of the mechanical energy required for each step and enhancing propulsion [42, 43]. Stretched plantar fascia adds stiffness to the medial and lateral arch and makes a situation to increase the arch height whereby the foot muscles (soleus, medial and lateral gastrocnemius) can create a high plantarflexion moment in order to propel the body forward [44, 45] and this issue will be reinforced by windlass mechanism. The windlass mechanism is based on the shortening of the plantar fascia due to hallux dorsiflexion [46, 47].

The hammer toe is one of the foot deformities. The area involved in this deformity is the proximal interphalangeal joint, bent downward, and the toes deviate from being aligned to the metatarsals in rest and unloading situations. This abnormality occurs with a probability between 2 and 20% of the toe deformities [48]. Despite various reports about the association of some foot deformities with subsequent damages in the foot, ankle, knee, and hip, there has not been a full investigation of the effect of hammer toe deformity on the joints, PF, and overall progressive detriment. The aim of this study is to indicate some of the hammer toe side effects on the lower limb, especially in PF, during walking using finite element and musculoskeletal modeling.

2. Method

2.1 Subjects

First participant was a male (age: 53, height: 165 cm, weight:93 Kg) with hammer toes deformity in the left foot and healthy contralateral foot (right foot). Second participant was healthy female (age: 25, height: 163 cm, weight:58 Kg) with no foot abnormalities volunteered for the study. They were recruited for gait analysis, and MRI imaging was done only on the male subject's left foot.

2.2 Gait analysis

Three-dimensional gait analysis was taken on both participants. 24 markers based on Vicon plug-in gait placement recommendations [49] and 14 extra markers as a modified plug-in gait were used [50–53]. The laboratory was equipped with 10 infrared cameras motion capture system (Vicon, Oxford, UK) with data

collection speed at 100 Hz. For collecting ground reaction forces (GRFs) and centre of pressure (COP), two force plates (Kistler, Winterthur, Switzerland) were occupied at 100 Hz sampling. For collecting the foot plantar pressure distribution, one pressure pad system (Payatek, Tehran, Iran) was employed. The electromyography (EMG) system was a 6-channel wireless Myon product (Schwarzenberg, Switzerland) located in line with SENIAM guidelines [54, 55]. Nexus software (Vicon, Oxford, UK) was responsible for collecting Kinematic data (marker trajectories), muscle activation signals, GRFs, and COP in synchronization. Muscles Activation were obtained from six major muscles: lateral gastrocnemius, tibialis anterior, soleus, medial gastrocnemius, tibialis posterior, and peroneus longus. In order to use the EMG's data, a five-step procedure consisting of some filters and math operations were used, as mentioned in the previous study [56]. Both participants were required to walk barefoot across the walkway at a normal speed. In addition to the dynamic trials repeated several times to ensure repeatability of gait analysis results, the static trial was collected.

2.3 Musculoskeletal modeling

The 'gait 2392' generic musculoskeletal model in OpenSim software was scaled using static trial data and the participant's body mass [57]. This general model consists of 92 musculotendon actuators, 10 rigid bodies with 23 degrees of freedom (DOF) was utilized for predicting joint reaction forces (JRFs) and muscle forces. After scaling, the inverse kinematic tool was used to reconstruct desired walking motion. Net moments and muscle forces were calculated using inverse dynamic and static optimization tools, respectively. The reactions between two contacting segments of the joints were determined using the Joint Reaction Analysis in OpenSim, which performs as a post-processor step whose input includes GRFs, muscle forces, and the output of the inverse kinematic. All of this input will be induced on the free body diagram of the scaled model segments for calculating the joint reactions [37, 58, 59]. The musculoskeletal model for the participant with hammer toe foot was validated in our previous study [60]. In order to validate the healthy participant model, muscle activation results in OpenSim software were compared to filtered and normalized similar signals of the EMG test. Comparing the pattern of the muscle activations shows a good agreement. Tibialis anterior and medial gastrocnemius muscle activations can be seen in Fig. A1 at appendix A.

3. Finite Element Modeling

The Mimics software (Materialise, Leuven, Belgium) was used to segment and generate a 3D soft and hard tissue model of the participant's left foot with hammer toe based on MRI medical images. A 1.5 T MRI scan (Philips Ingenia, spacing between slices: 0.5 mm and slice thickness: 1 mm, sequence 3D mDion Te Hr, TE/TR 9/29) was performed on the left foot in an unloaded position. Pads and cushions kept the leg and foot at a 90 degree angle. The model had 30 bones (medial and lateral sesamoids, 14 phalanges, 5 metatarsals, cuboid, 3 cuneiforms, navicular, calcaneus, talus, and the distal sections of the tibia and fibula) and a bulk of soft tissue. 74 cartilage layers for 37 pairs of joints were incorporated to increase the model's accuracy. Surface-to-surface frictionless contact was used to describe the interaction between cartilage layers.

To perform the finite element analysis, all components were imported into ABAQUS software (SIMULIA, Providence, USA). The ligaments are not clearly defined in MRI scans. So, 2174 truss elements were added to the model to identify key ligaments and the plantar fascia which were placed using anatomical atlases [61]. Achilles tendon tied on top of the calcaneus (see fig. 1). soft tissue encased all of the other components by embedding the bones, cartilages, ligaments, and Achilles tendon in to the bulk of the soft tissue. The ground was represented by a 3D rigid rectangular plate. Based on previous research, contact between the plate and the sole of the foot was regarded surface to surface with a frictional coefficient of 0.6 [62]. According to the literature, the material properties of all components were considered to be as shown in Table 1 [63, 64].

3.1 Walking simulation:

Under quasi-static analysis, five instants (heel strike, early stance, midstance, late stance, and toe-off) of a stance phase throughout the gait cycle were performed. The GRFs and muscle forces were applied to the model at each event. During the analysis, the top surface of the soft tissue, distal tibia, and fibula were fixed as boundary conditions. GRFs were applied to the ground plate at COP. The proper placement of COP on the model was determined according to the relative location of anatomical landmarks and COP. Six muscle forces were applied to the model. The forces of the soleus, medial, and lateral gastrocnemius were applied to the Achilles tendon, and the force of the tibialis anterior, tibialis posterior, and peroneus longus, were allocated to their relevant bones along the muscle force vectors defined by the OpenSim model. [8, 65].

4. Result

Comparison between the results of the plantar fascia tension force during walking obtained by finite element (FE) modeling of HTF in the current study, Chen et al. [66], and Erdemir et al. [41] are shown in Fig. 2. Muscle forces obtained by Opensim for major active muscle in the propulsion of walking are shown in Fig. 3. As mentioned in section 3, FE modeling only was performed for the left hammer toe foot. Figure 4 shows the results of lateral/medial displacement of forefoot bones during the four events of stance phase predicted by finite element modeling. The results of the stress distribution in bony structure and also plantar and internal von Mises stress distribution in sagittal plane view are shown in the Fig. 5. It should be noted that the FE model was previously validated by comparing the predicted plantar pressure and the pressure pad results [60].

Results of plantar fascia stresses are shown in Fig. 6. After presenting the results in the sole, the question is whether changes in the location of the COP and the areas involved in weight-bearing due to hammer toe could affect the performance of other parts, such as the joints. For this aim, the results of the foot joint reactions during the walking are presented in Figs. 7 and Appendix B for two participants, healthy and hammer toe foot. Forces and moments direction are based on coordinate shown in Fig. 1.

Table 1
material property of the all parts [63, 64] and element type of the components

Components	Young's modulus (MPa)	Poisson's ratio	Cross section (mm^2)	Element Type
Hard tissue (bones)	7300	0.3	–	Tetrahedral
Ligament	260	–	18.4	Truss
Cartilage	1	0.4	–	Tetrahedral
Plantar fascia	350	–	290.7	Truss
Ground support	17000	0.1	–	Linear hexahedral
Achilles tendon	816	3.0	–	Tetrahedral
Encapsulated soft tissue	Hyperelastic (second-order polynomial strain energy potential equation, C_{10} = 0.08556 Nmm^{-2},C_{01} = -0.05841 Nmm^{-2}, C_{20} = 0.03900 Nmm^{-2}, C_{11} = -0.02319 Nmm^{-2}, C_{02} = 0.00851 Nmm^{-2},D_1 = 3.65273 mm^2N^{-1}, D_2 = 0.0000 mm^2N^{-1})			Tetrahedral

5. Discussion

The hammer toe is one of the relatively common deformities at the foot. Investigation of hammer toe side effects on the other parts of the lower limb can be helpful for better identification of this deformity as well as prevention of progressive pain. For this aim, the finite element model including soft and hard tissue, ligament, and cartilage were used as well as musculoskeletal modeling. The validation of the finite element results was performed by comparing the results of the predicted plantar pressure distribution of the foot with the results of the experimental pressure pad at previous study [60]. In order to validate musculoskeletal model, the results of the predicted intensity of muscle activities were compared with EMG signals.

As our previous study [60] and soft tissue von Mises stress distribution in Fig. 5 show, the presence of a hammer toe, not only causes the stress concentration in the forefoot, but also will increase plantar pressure and internal stresses and will increase the risk of injury and ulcers. In the present study, it is tried to show the other aspects of hammer toe deformity effects on the lower limb.

Wang et al. [67] showed that body weight force (BWF) transmits by the medial metatarsals (1st, 2nd, and 3rd toes and metatarsals), which is in line with the peak plantar pressure region in Akrami et al. [8] results. In addition, Kalra et al. [68] showed the important role of medial metatarsals, especially the second one in BWF transmission by investigating on 10 cadaveric feet. As shown in Fig. 5, the hammer toe changes the location of transfer body weight force line to the lateral side of the foot, and the 3rd, 4th, and 5th

metatarsal had a significant function in weight-bearing. The function of several parts of the lower limb may be affected as a result of this condition. Previous researches on healthy feet found that fifth metatarsal has lower maximum stress compared to other metatarsals [67, 69, 70] while fifth metatarsal fractures are thought to occur more frequently than any other metatarsal fractures [71], while the hammertoe increased stress in the fifth metatarsal, indicating an increased risk of fifth metatarsal fracture. In Fig. 4, the results of lateral/medial displacement of hammer toe foot show that the displacement of the little toe, especially in the metatarsal region, is considerable and indicates expectancy and the probability of bunionette (tailor's bunion) as the subsequent possible deformity. At the same time, the results of the stress distribution, as well as the displacement of the first toe in the MTP joint, do not demonstrate the possibility of Bunions (Hallux Valgus), as a side effect of the hammer toe.

The contact area of the foot with the ground is reduced when the hammer toe occurs, and the toes are less involved in weight bearing during walking. As shown in Fig. 7, MTP joint reaction force for hammer toe foot is less than the healthy foot, and also the stress distribution results in Fig. 5 indicate the significant difference between metatarsals and toes stress, and this issue shows a shift in the contribution of the toes in weight bearing to the metatarsals. Furthermore, this means a reduction in foot length which acts flat spring-like. The stiffness of the flat spring rises as its length decreases, so the hammer toe exhibit more rigid foot, and this condition has an impact on the lower limb's induced forces. A rigid foot is less likely to be able to absorb shocks, resulting in intense ground forces being imposed on the foot [72, 73]. Rigid foot causes higher ankle, knee, and hip joint reaction forces, which in this study appeared in knee forces with 50% higher than a healthy foot and also disappearing the double hump in vertical knee and hip reaction forces that were monotonically increasing in most of the stance phase, as shown in figures B1 and B2 at appendix B.

The results of the joint reactions indicate the distinction of the knee abduction moment pattern, as well as the amount of force on the knee and hip between hammer toe and healthy foot as shown in Appendix A. Our results of the healthy foot (pattern and magnitude) are in line with previous studies [74, 75]. A notable point on the peak of the reaction moments is that since the hammer toe shifted the position of the COP to the lateral, the moment arm of the total GRFs has been reduced on joints, which is aligned with the previous finding [76]. For this reason, the peak reaction moments for hammer toe foot are lower than the healthy foot.

Based on the plantar fascia tension shown in Fig. 6, the productivity of plantar capacity does not occur in the hammer toe foot, and as a result, there is less shock and energy absorption in the plantar fascia of the hammer toe foot. Caravaggi et al. [77] showed that the overall tensional plantar fascia load decreases from medial to lateral in healthy foot and also the previous studies showed that the medial side of the plantar has higher stress during walking [78], and the medial side was reported as maximum stress area [44, 66] which show that hallux plantar ray has a significant role in elastic energy storage. On the other hand, plantar fasciitis occurs as a consequence of excess mechanical load on the fascia [79, 80]. Results of this study show that for the hammer toe as the deformity and consequent poor windlass mechanism, the maximum tensional load does not occur at the medial side of the plantar fascia, and the first ray of

the plantar fascia under the 1st MTP has lower tensile force during walking shown in Fig. 6. Furthermore, the result of PF stresses shows as well as 2nd plantar ray, lateral side of the PF is expected to be more prone to the onset of small tears and injury in HTF as a result of the continues forces induced during the stance phase of gait. The need for more muscular forces will be reduced by storing energy in tendons and ligaments during walking [42, 81, 82] expected up to 17% of the overall mechanical energy spent during walking [83]. As shown in Fig. 3, due to reduction of the elastic stored energy at the PF, required power and muscle forces for HMT foot is higher than HF, and this issue raises metabolic cost. The soleus, medial and lateral gastrocnemius make a contribution to 93 percent of the plantar flexion torque during a step [84]. The tensions in the Achilles tendon and plantar fascia are mechanically connected. Increasing the PF tension, in addition to providing integrity to the bony arch structure, increases the tension in the Achilles tendon, which is likely to reduce the metabolic cost of walking [85]. As shown in Fig. 2, PF force significantly reduced in HMT foot, and as shown in Fig. 3, this issue demands extra soleus, medial and lateral gastrocnemius muscle force for effective propulsion and this matter makes the body use more energy during walking.

According to Zhang et al. [86], injuries in joints, such as the knee joint and osteoarthritis, will increase the force induced on foot. Also based on the results of soft tissue stress distribution shown in Fig. 5, deformity at the metatarsal head makes the stress concentration and increases internal and plantar stresses in hammer toe foot which is consistent with previous studies [22, 60].

6. Conclusion

The hammer toe deformity was found to change the pattern and line of bodyweight force transmission and also affects the forces and moments of the joints. Also, this study revealed that hammer toe deformity makes dorsiflexion of the toes and the windlass mechanism less effective during walking. Specifically, the FE results showed that plantar fascia (PF) in HTF played a less dominant role in bearing load in comparison with HF. Also, the results indicated that the stored elastic energy in PF was less in HTF compared to the HF, which can indicate a metabolic cost during walking. Stresses in the plantar fascia element for HTF shows not only the medial part but also the lateral part is exposed to plantar fasciitis. Internal stress distribution shows that the majority of bodyweight force is transmitted through the lateral metatarsals in hammer toe foot, and the probability of fifth metatarsal fracture and also progressive deformity like tailor's bunion was subsequently increased. The MSM results show the joint reaction forces and moments in the hammer toe foot have deviated from the normal function which the intensity of the metatarsophalangeal joint reactions in hammer toe are less than the healthy foot, HTF joint forces have a more extended period with monotonically increasing intensity during the stance phase in comparison to HF. In this way, a cycle can be indicated between five parameters: foot deformity, increased plantar pressure, stress concentration and increased internal stresses, change in body weight force transmission line, and deviation of joint reactions and plantar fascia from normal manner.

Consequently, it can be stated that a cycle between deformity, stress concentration and increased internal stresses, changes in BWF transmission line, joint malfunction and increased plantar pressures are

established in hammer toe foot that can lead to an increase in the risk of ulceration for the diabetic foot (figure C1).

References

1. D. R. Bonanno, K. B. Landorf, S. E. Munteanu, G. S. Murley, and H. B. Menz, "Effectiveness of foot orthoses and shock-absorbing insoles for the prevention of injury: a systematic review and meta-analysis," British journal of sports medicine, vol. 51, pp. 86–96, 2017.
2. D. Murphy, D. Connolly, and B. Beynnon, "Risk factors for lower extremity injury: a review of the literature," British journal of sports medicine, vol. 37, pp. 13–29, 2003.
3. B. S. Neal, I. B. Griffiths, G. J. Dowling, G. S. Murley, S. E. Munteanu, M. M. F. Smith, *et al.*, "Foot posture as a risk factor for lower limb overuse injury: a systematic review and meta-analysis," Journal of foot and ankle research, vol. 7, pp. 1–13, 2014.
4. F. G. Neely, "Intrinsic risk factors for exercise-related lower limb injuries," Sports medicine, vol. 26, pp. 253–263, 1998.
5. A. K. Wills, *Gait kinematics and risk factors for overuse anterior knee pain*: University of Surrey (United Kingdom), 2006.
6. D. L. López, L. C. González, M. E. L. Iglesias, J. L. S. Canosa, D. R. Sanz, C. C. Lobo, *et al.*, "Quality of life impact related to foot health in a sample of older people with hallux valgus," Aging and disease, vol. 7, p. 45, 2016.
7. A. Scarton, A. Guiotto, T. Malaquias, F. Spolaor, G. Sinigaglia, C. Cobelli, *et al.*, "A methodological framework for detecting ulcers' risk in diabetic foot subjects by combining gait analysis, a new musculoskeletal foot model and a foot finite element model," Gait & posture, vol. 60, pp. 279–285, 2018.
8. M. Akrami, Z. Qian, Z. Zou, D. Howard, C. J. Nester, and L. Ren, "Subject-specific finite element modelling of the human foot complex during walking: sensitivity analysis of material properties, boundary and loading conditions," Biomechanics and modeling in mechanobiology, vol. 17, pp. 559–576, 2018.
9. B. J. Chun and I. G. Jang, "Determination of the representative static loads for cyclically repeated dynamic loads: a case study of bone remodeling simulation with gait loads," Computer Methods and Programs in Biomedicine, vol. 200, p. 105924, 2021.
10. T. A. Wren, C. A. Tucker, S. A. Rethlefsen, G. E. Gorton III, and S. Õunpuu, "Clinical efficacy of instrumented gait analysis: Systematic review 2020 update," Gait & posture, vol. 80, pp. 274–279, 2020.
11. Y. Sun, S. Liang, Y. Yu, Y. Yang, J. Lu, J. Wu, *et al.*, "Plantar Pressure-Based Temporal Analysis of Gait Disturbance in Idiopathic Normal Pressure Hydrocephalus: Indications from A Pilot Longitudinal Study," *Computer Methods and Programs in Biomedicine*, p. 106691, 2022.

12. J. P. Charles, F. Suntaxi, and W. J. Anderst, "In vivo human lower limb muscle architecture dataset obtained using diffusion tensor imaging," PloS one, vol. 14, p. e0223531, 2019.
13. H. Partsch, M. Clark, S. Bassez, J. P. BENIGNI, F. Becker, V. Blazek, *et al.*, "Measurement of lower leg compression in vivo: recommendations for the performance of measurements of interface pressure and stiffness," *Dermatologic surgery*, vol. 32, pp. 224–233, 2006.
14. D. B. Burr, C. Milgrom, D. Fyhrie, M. Forwood, M. Nyska, A. Finestone, *et al.*, "In vivo measurement of human tibial strains during vigorous activity," *Bone*, vol. 18, pp. 405–410, 1996.
15. T.-W. Lu, J. J. O'Connor, S. J. Taylor, and P. S. Walker, "Validation of a lower limb model with in vivo femoral forces telemetered from two subjects," Journal of biomechanics, vol. 31, pp. 63–69, 1997.
16. A. Healy, R. Naemi, and N. Chockalingam, "The effectiveness of footwear as an intervention to prevent or to reduce biomechanical risk factors associated with diabetic foot ulceration: a systematic review," Journal of Diabetes and its Complications, vol. 27, pp. 391–400, 2013.
17. E. J. Boyko, J. H. Ahroni, V. Stensel, R. C. Forsberg, D. R. Davignon, and D. G. Smith, "A prospective study of risk factors for diabetic foot ulcer. The Seattle Diabetic Foot Study," *Diabetes care*, vol. 22, pp. 1036–1042, 1999.
18. B. Iraj, F. Khorvash, A. Ebneshahidi, and G. Askari, "Prevention of diabetic foot ulcer," International journal of preventive medicine, vol. 4, p. 373, 2013.
19. Q. Zhou, M. Peng, L. Zhou, J. Bai, A. Tong, M. Liu, *et al.*, "Development and validation of a brief diabetic foot ulceration risk checklist among diabetic patients: a multicenter longitudinal study in China," Scientific reports, vol. 8, pp. 1–8, 2018.
20. B. H. M. Tan, A. Nather, and V. David, "Biomechanics of the foot," in *Diabetic Foot Problems*, ed: World Scientific, 2008, pp. 67–75.
21. J. Bevans, "Biomechanics and plantar ulcers in diabetes," The Foot, vol. 2, pp. 166–172, 1992.
22. S. A. Bus, M. Maas, A. de Lange, R. P. Michels, and M. Levi, "Elevated plantar pressures in neuropathic diabetic patients with claw/hammer toe deformity," Journal of biomechanics, vol. 38, pp. 1918–1925, 2005.
23. X. Yu, G. Yu, Y. Chen, and X. Liu, "The characteristics and clinical significance of plantar pressure distribution in patients with diabetic toe deformity: a dynamic plantar pressure analysis," Journal of International Medical Research, vol. 39, pp. 2352–2359, 2011.
24. S. Gnanasundaram, P. Ramalingam, B. N. Das, and V. Viswanathan, "Gait changes in persons with diabetes: Early risk marker for diabetic foot ulcer," Foot and Ankle Surgery, vol. 26, pp. 163–168, 2020.
25. K. D. Gross, D. T. Felson, J. Niu, D. J. Hunter, A. Guermazi, F. W. Roemer, *et al.*, "Flat feet are associated with knee pain and cartilage damage in older adults," Arthritis care & research, vol. 63, 2011.
26. J. W. Tong and P. W. Kong, "Association between foot type and lower extremity injuries: systematic literature review with meta-analysis," journal of orthopaedic & sports physical therapy, vol. 43, pp. 700–714, 2013.

27. Y. Peng, W. Niu, D. W.-C. Wong, Y. Wang, T. L.-W. Chen, G. Zhang, *et al.*, "Biomechanical comparison among five mid/hindfoot arthrodeses procedures in treating flatfoot using a musculoskeletal multibody driven finite element model," Computer Methods and Programs in Biomedicine, vol. 211, p. 106408, 2021.
28. K.-S. Shih, H.-L. Chien, T.-W. Lu, C.-F. Chang, and C.-C. Kuo, "Gait changes in individuals with bilateral hallux valgus reduce first metatarsophalangeal loading but increase knee abductor moments," Gait & posture, vol. 40, pp. 38–42, 2014.
29. N. Steinberg, A. Finestone, M. Noff, A. Zeev, and G. Dar, "Relationship between lower extremity alignment and hallux valgus in women," Foot & ankle international, vol. 34, pp. 824–831, 2013.
30. R. Woźniacka, Ł. Oleksy, A. Jankowicz-Szymańska, A. Mika, R. Kielnar, and A. Stolarczyk, "The association between high-arched feet, plantar pressure distribution and body posture in young women," Scientific reports, vol. 9, pp. 1–9, 2019.
31. R. Zifchock, R. Parker, W. Wan, M. Neary, J. Song, and H. Hillstrom, "The relationship between foot arch flexibility and medial-lateral ground reaction force distribution," Gait & posture, vol. 69, pp. 46–49, 2019.
32. C. P. Ojukwu, E. G. Anyanwu, and G. G. Nwafor, "Correlation between foot arch index and the intensity of foot, knee, and lower back pain among pregnant women in a south-eastern nigerian community," Medical Principles and Practice, vol. 26, pp. 480–484, 2017.
33. C. R. Winby, D. G. Lloyd, T. F. Besier, and T. B. Kirk, "Muscle and external load contribution to knee joint contact loads during normal gait," Journal of biomechanics, vol. 42, pp. 2294–2300, 2009.
34. G. Valente, L. Pitto, D. Testi, A. Seth, S. L. Delp, R. Stagni, *et al.*, "Are subject-specific musculoskeletal models robust to the uncertainties in parameter identification?," PLoS One, vol. 9, p. e112625, 2014.
35. A. Karatsidis, M. Jung, H. M. Schepers, G. Bellusci, M. de Zee, P. H. Veltink, *et al.*, "Predicting kinetics using musculoskeletal modeling and inertial motion capture," *arXiv preprint arXiv:1801.01668*, 2018.
36. R. L. Thompson, J. K. Gardner, S. Zhang, and J. A. Reinbolt, "Lower-limb joint reaction forces and moments during modified cycling in healthy controls and individuals with knee osteoarthritis," Clinical Biomechanics, vol. 71, pp. 167–175, 2020.
37. K. M. Steele, M. S. DeMers, M. H. Schwartz, and S. L. Delp, "Compressive tibiofemoral force during crouch gait," Gait & posture, vol. 35, pp. 556–560, 2012.
38. B. A. Knarr and J. S. Higginson, "Practical approach to subject-specific estimation of knee joint contact force," Journal of biomechanics, vol. 48, pp. 2897–2902, 2015.
39. J. T.-M. Cheung, K.-N. An, and M. Zhang, "Consequences of partial and total plantar fascia release: a finite element study," Foot & ankle international, vol. 27, pp. 125–132, 2006.
40. S. C. Wearing, J. E. Smeathers, S. R. Urry, E. M. Hennig, and A. P. Hills, "The pathomechanics of plantar fasciitis," Sports medicine, vol. 36, pp. 585–611, 2006.
41. A. Erdemir, A. J. Hamel, A. R. Fauth, S. J. Piazza, and N. A. Sharkey, "Dynamic loading of the plantar aponeurosis in walking," *JBJS*, vol. 86, pp. 546–552, 2004.

42. K. A. McDonald, S. M. Stearne, J. A. Alderson, I. North, N. J. Pires, and J. Rubenson, "The role of arch compression and metatarsophalangeal joint dynamics in modulating plantar fascia strain in running," PloS one, vol. 11, p. e0152602, 2016.
43. L. A. Kelly, A. G. Cresswell, and D. J. Farris, "The energetic behaviour of the human foot across a range of running speeds," Scientific reports, vol. 8, pp. 1–6, 2018.
44. H.-Y. K. Cheng, C.-L. Lin, H.-W. Wang, and S.-W. Chou, "Finite element analysis of plantar fascia under stretch—the relative contribution of windlass mechanism and Achilles tendon force," Journal of biomechanics, vol. 41, pp. 1937–1944, 2008.
45. E. D. Ward, K. M. Smith, J. R. Cocheba, P. E. Patterson, and R. D. Phillips, "In vivo forces in the plantar fascia during the stance phase of gait: sequential release of the plantar fascia," Journal of the American Podiatric Medical Association, vol. 93, pp. 429–442, 2003.
46. L. Welte, L. A. Kelly, G. A. Lichtwark, and M. J. Rainbow, "Influence of the windlass mechanism on arch-spring mechanics during dynamic foot arch deformation," Journal of the Royal Society Interface, vol. 15, p. 20180270, 2018.
47. H.-Y. K. Cheng, C.-L. Lin, S.-W. Chou, and H.-W. Wang, "Nonlinear finite element analysis of the plantar fascia due to the windlass mechanism," Foot & ankle international, vol. 29, pp. 845–851, 2008.
48. J. Schrier, "Forefoot disorders: definitions, treatment and outcome measurement," 2017.
49. (2021, Accessed 14 January 2021). Available: https://docs.vicon.com/display/Nexus211/PDF+downloads+for+Vicon+Nexus
50. F. Stief, H. Böhm, K. Michel, A. Schwirtz, and L. Döderlein, "Reliability and accuracy in three-dimensional gait analysis: a comparison of two lower body protocols," Journal of applied biomechanics, vol. 29, pp. 105–111, 2013.
51. P. J. Renaud, *Three-dimensional kinematics of the lower limbs during ice hockey skating starts on the ice surface*: McGill University (Canada), 2016.
52. E. Flux, M. van der Krogt, P. Cappa, M. Petrarca, K. Desloovere, and J. Harlaar, "The Human Body Model versus conventional gait models for kinematic gait analysis in children with cerebral palsy," Human movement science, vol. 70, p. 102585, 2020.
53. A. Leardini, M. G. Benedetti, L. Berti, D. Bettinelli, R. Nativo, and S. Giannini, "Rear-foot, mid-foot and fore-foot motion during the stance phase of gait," Gait & posture, vol. 25, pp. 453–462, 2007.
54. H. J. Hermens, B. Freriks, R. Merletti, D. Stegeman, J. Blok, G. Rau, *et al.*, "European recommendations for surface electromyography," Roessingh research and development, vol. 8, pp. 13–54, 1999.
55. S. McGill, D. Juker, and P. Kropf, "Appropriately placed surface EMG electrodes reflect deep muscle activity (psoas, quadratus lumborum, abdominal wall) in the lumbar spine," Journal of biomechanics, vol. 29, pp. 1503–1507, 1996.
56. M. Baniasad, F. Farahmand, M. Arazpour, and H. Zohoor, "Coordinated activities of trunk and upper extremity muscles during walker-assisted paraplegic gait: A synergy study," Human movement science, vol. 62, pp. 184–193, 2018.

57. S. L. Delp, F. C. Anderson, A. S. Arnold, P. Loan, A. Habib, C. T. John, *et al.*, "OpenSim: open-source software to create and analyze dynamic simulations of movement," IEEE transactions on biomedical engineering, vol. 54, pp. 1940–1950, 2007.
58. A. Seth, M. Sherman, J. A. Reinbolt, and S. L. Delp, "OpenSim: a musculoskeletal modeling and simulation framework for in silico investigations and exchange," Procedia Iutam, vol. 2, pp. 212–232, 2011.
59. M. S. DeMers, S. Pal, and S. L. Delp, "Changes in tibiofemoral forces due to variations in muscle activity during walking," Journal of orthopaedic research, vol. 32, pp. 769–776, 2014.
60. M. Moayedi, A. Arshi, M. Salehi, M. Akrami, and R. Naemi, "Associations between changes in loading pattern, deformity, and internal stresses at the foot with hammer toe during walking; a finite element approach," Computers in Biology and Medicine, vol. 135, p. 104598, 2021.
61. R. Drake, A. W. Vogl, A. W. Mitchell, R. Tibbitts, and P. Richardson, *Gray's Atlas of Anatomy E-Book*: Elsevier Health Sciences, 2020.
62. M. Zhang and A. Mak, "In vivo friction properties of human skin," Prosthetics and orthotics International, vol. 23, pp. 135–141, 1999.
63. J. T.-M. Cheung, M. Zhang, A. K.-L. Leung, and Y.-B. Fan, "Three-dimensional finite element analysis of the foot during standing—a material sensitivity study," Journal of biomechanics, vol. 38, pp. 1045–1054, 2005.
64. C. Mkandawire, W. R. Ledoux, B. J. Sangeorzan, and R. P. Ching, "Foot and ankle ligament morphometry," Journal of Rehabilitation Research & Development, vol. 42, 2005.
65. Z.-h. Qian, L. Ren, L.-q. Ren, and A. Boonpratatong, "A three-dimensional finite element musculoskeletal model of the human foot complex," in *6th World Congress of Biomechanics (WCB 2010). August 1–6, 2010 Singapore*, 2010, pp. 297–300.
66. Y.-N. Chen, C.-W. Chang, C.-T. Li, C.-H. Chang, and C.-F. Lin, "Finite element analysis of plantar fascia during walking: a quasi-static simulation," Foot & ankle international, vol. 36, pp. 90–97, 2015.
67. Y. Wang, Z. Li, D. W.-C. Wong, C.-K. Cheng, and M. Zhang, "Finite element analysis of biomechanical effects of total ankle arthroplasty on the foot," Journal of orthopaedic translation, vol. 12, pp. 55–65, 2018.
68. M. Kalra, R. Bahensky, S. D. McLachlin, D. S. Cronin, and N. Chandrashekar, "In-Situ Fracture Tolerance of the Metatarsals During Quasi-Static Compressive Loading of the Human Foot," Journal of Biomechanical Engineering, vol. 144, 2022.
69. J. M. García-Aznar, J. Bayod, A. Rosas, R. Larrainzar, R. García-Bógalo, M. Doblaré, *et al.*, "Load transfer mechanism for different metatarsal geometries: a finite element study," Journal of biomechanical engineering, vol. 131, 2009.
70. Y. Gu, X. Ren, J. Li, M. Lake, Q. Zhang, and Y. Zeng, "Computer simulation of stress distribution in the metatarsals at different inversion landing angles using the finite element method," International orthopaedics, vol. 34, pp. 669–676, 2010.

71. J. M. Kane, K. Sandrowski, H. Saffel, A. Albanese, S. M. Raikin, and D. I. Pedowitz, "The epidemiology of fifth metatarsal fracture," Foot & ankle specialist, vol. 8, pp. 354–359, 2015.
72. D. S. Williams Iii, I. S. McClay, and J. Hamill, "Arch structure and injury patterns in runners," Clinical biomechanics, vol. 16, pp. 341–347, 2001.
73. S. Subotnick and P. Sisney, "Treatment of Achilles tendinopathy in the athlete," Journal of the American Podiatric Medical Association, vol. 76, pp. 552–557, 1986.
74. M. Baniasad, M. S. Fard, F. Farahmand, and K. Aminian, "Can the ground reaction vector be an alternative to conventional gait model to estimate knee adduction moment?," Gait & Posture, vol. 81, pp. 24–25, 2020.
75. B. A. Sanford, J. L. Williams, A. R. Zucker-Levin, and W. M. Mihalko, "Hip, knee, and ankle joint forces in healthy weight, overweight, and obese individuals during walking," in *Computational biomechanics for medicine*, ed: Springer, 2014, pp. 101–111.
76. B. Ulrich, L. Hoffmann, B. M. Jolles, and J. Favre, "Changes in ambulatory knee adduction moment with lateral wedge insoles differ with respect to the natural foot progression angle," Journal of biomechanics, vol. 103, p. 109655, 2020.
77. P. Caravaggi, T. Pataky, J. Y. Goulermas, R. Savage, and R. Crompton, "A dynamic model of the windlass mechanism of the foot: evidence for early stance phase preloading of the plantar aponeurosis," Journal of Experimental Biology, vol. 212, pp. 2491–2499, 2009.
78. S.-C. Lin, C. P.-C. Chen, S. F.-T. Tang, C.-W. Chen, J.-J. Wang, C.-C. Hsu, *et al.*, "Stress distribution within the plantar aponeurosis during walking—a dynamic finite element analysis," Journal of Mechanics in Medicine and Biology, vol. 14, p. 1450053, 2014.
79. A. Aquino and C. Payne, "Function of the plantar fascia," The foot, vol. 9, pp. 73–78, 1999.
80. M. R. Hedrick, "The plantar aponeurosis," Foot & ankle international, vol. 17, pp. 646–649, 1996.
81. G. A. Cavagna, F. P. Saibene, and R. Margaria, "Mechanical work in running," Journal of applied physiology, vol. 19, pp. 249–256, 1964.
82. G. A. Cavagna, N. C. Heglund, and C. R. Taylor, "Mechanical work in terrestrial locomotion: two basic mechanisms for minimizing energy expenditure," *American Journal of Physiology-Regulatory, Integrative and Comparative Physiology*, vol. 233, pp. R243-R261, 1977.
83. R. Ker, M. Bennett, S. Bibby, R. Kester, and R. Alexander, "The spring in the arch of the human foot," Nature, vol. 325, pp. 147–149, 1987.
84. V. L. Giddings, G. S. BEAUPRÉ, R. T. WHALEN, and D. R. CARTER, "Calcaneal loading during walking and running," Medicine & Science in Sports & Exercise, vol. 32, pp. 627–634, 2000.
85. K. A. Kirby, "Longitudinal arch load-sharing system of the foot," Revista Española de Podología, vol. 28, pp. e18-e26, 2017.
86. Z. Zhang, L. Wang, K. Hu, and Y. Liu, "Characteristics of plantar loads during walking in patients with knee osteoarthritis," Medical science monitor: international medical journal of experimental and clinical research, vol. 23, p. 5714, 2017.

Figures

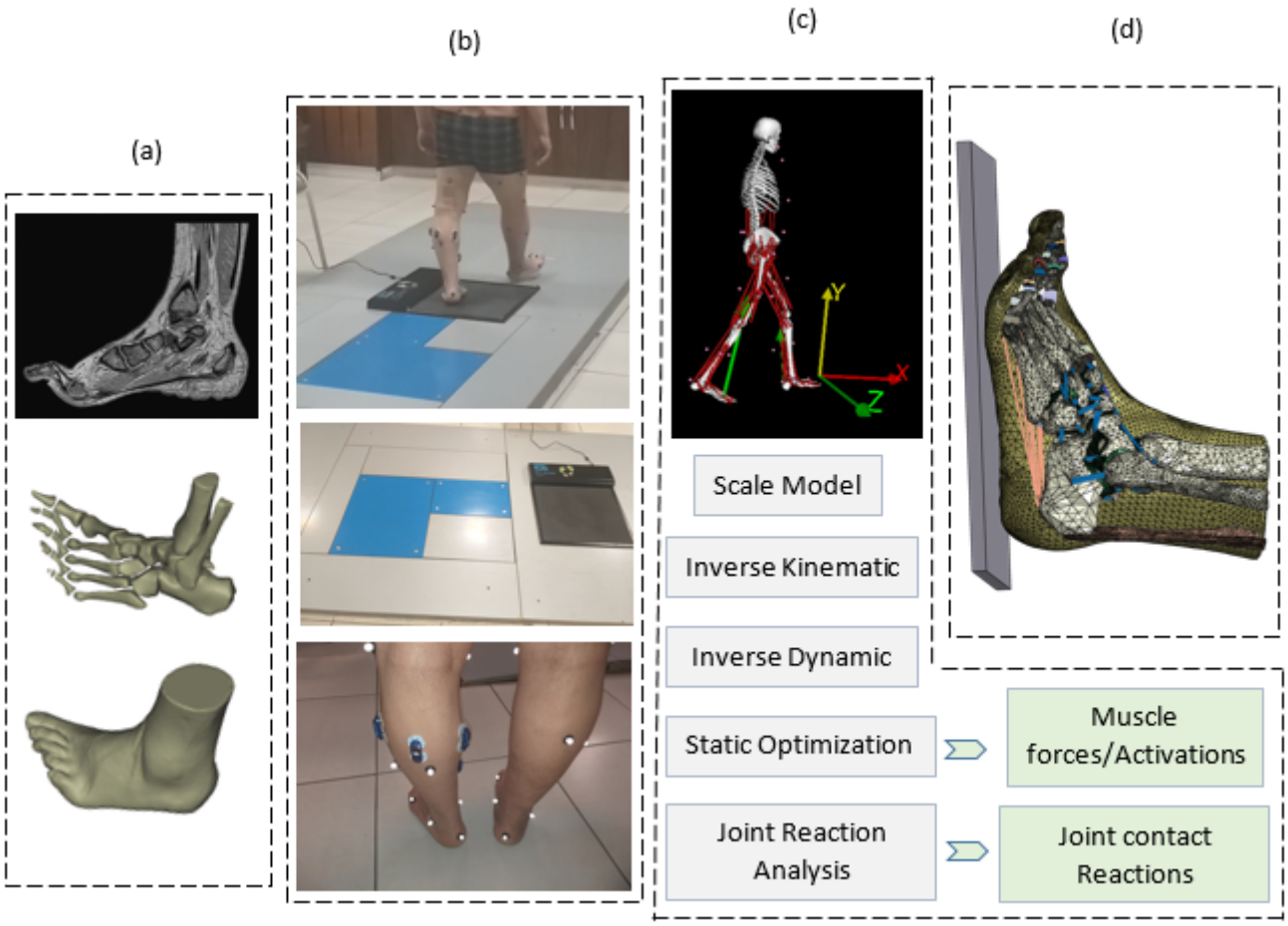

Figure 1

A summary of the steps processed in this study. (a) MRI imaging segmentation in Mimics software for 3D foot model construction (b) Gait analysis (c) Musculoskeletal modeling with Opensim software (d) importing the models into Abaqus software based on foot angles calculated by Vicon software and also inducing the boundary conditions for finite element analysis.

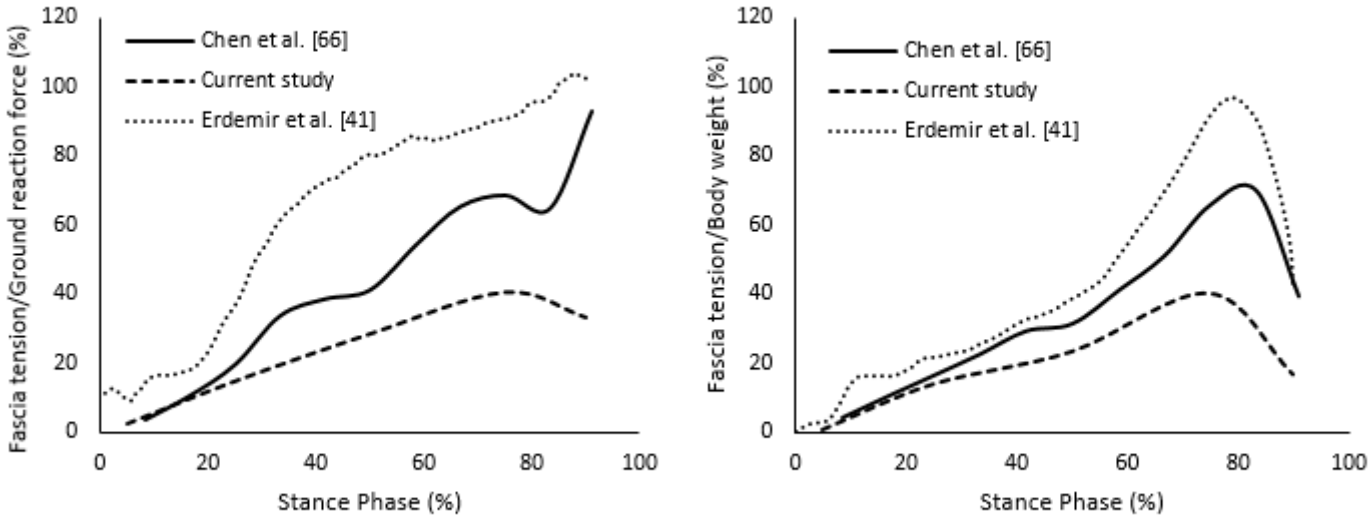

Figure 2

Total tension force induced on plantar fascia normalized by ground reaction force and body weight. The healthy foot study results by Chen et al. [66] and Erdemir et al. [41] were plotted for comparison.

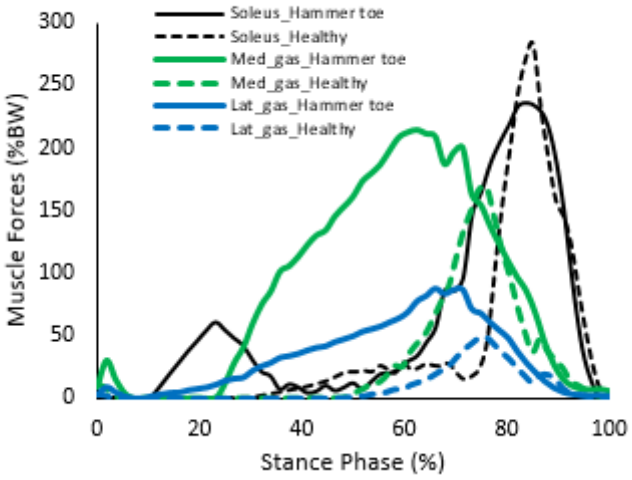

Figure 3

Selective muscle forces during walking. Soleus, medial and lateral gastrocnemius are the major active muscles in propulsion.

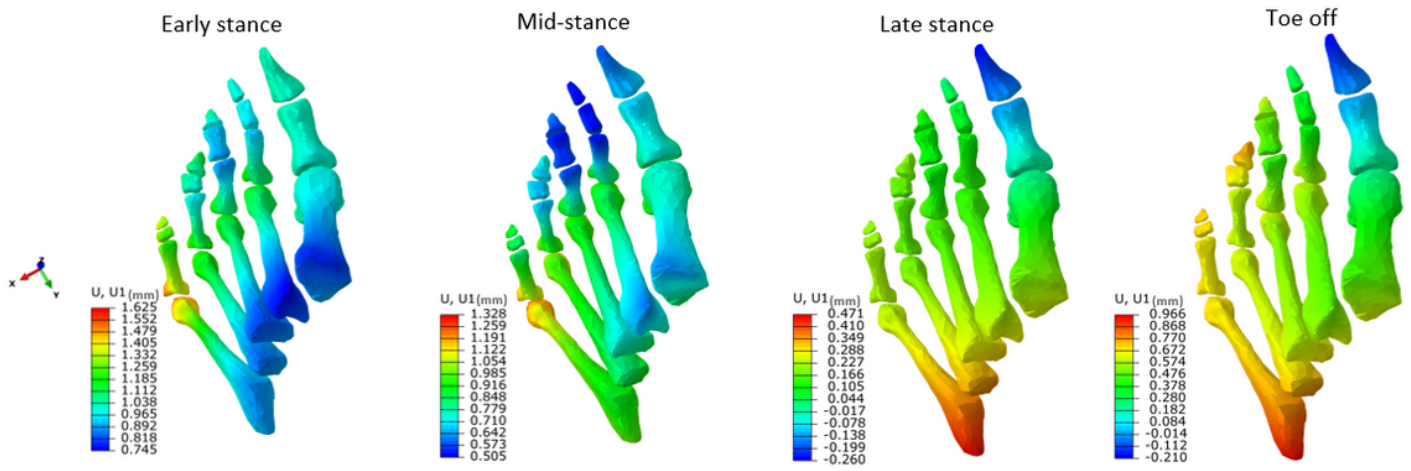

Figure 4

Lateral/medial displacement in hard tissues of hammer toe forefoot at for different events (a) Early stance (b) Mid-stance (c) Late stance (d) Toe off. The result of the heel strike was negligible in comparison to the four other events.

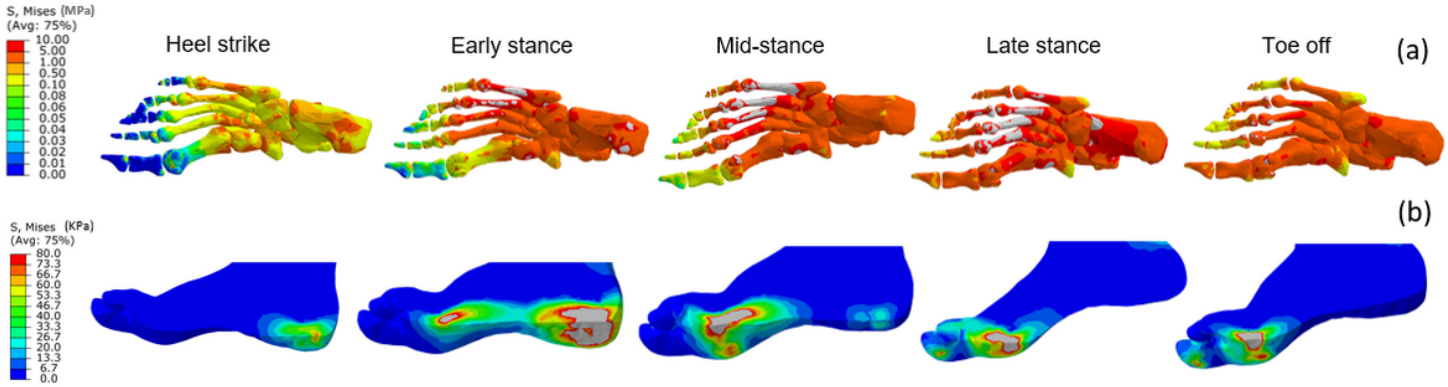

Figure 5

FE simulated internal stress distribution of hammer toe foot at five different events in (a) hard tissues which Light grey colour shows the von Mises higher than 10 (MPa). (b) View cut of soft tissue plantar and internal von Mises stress distribution at HMT foot. Light grey colour shows the von Mises higher than 80 (KPa)

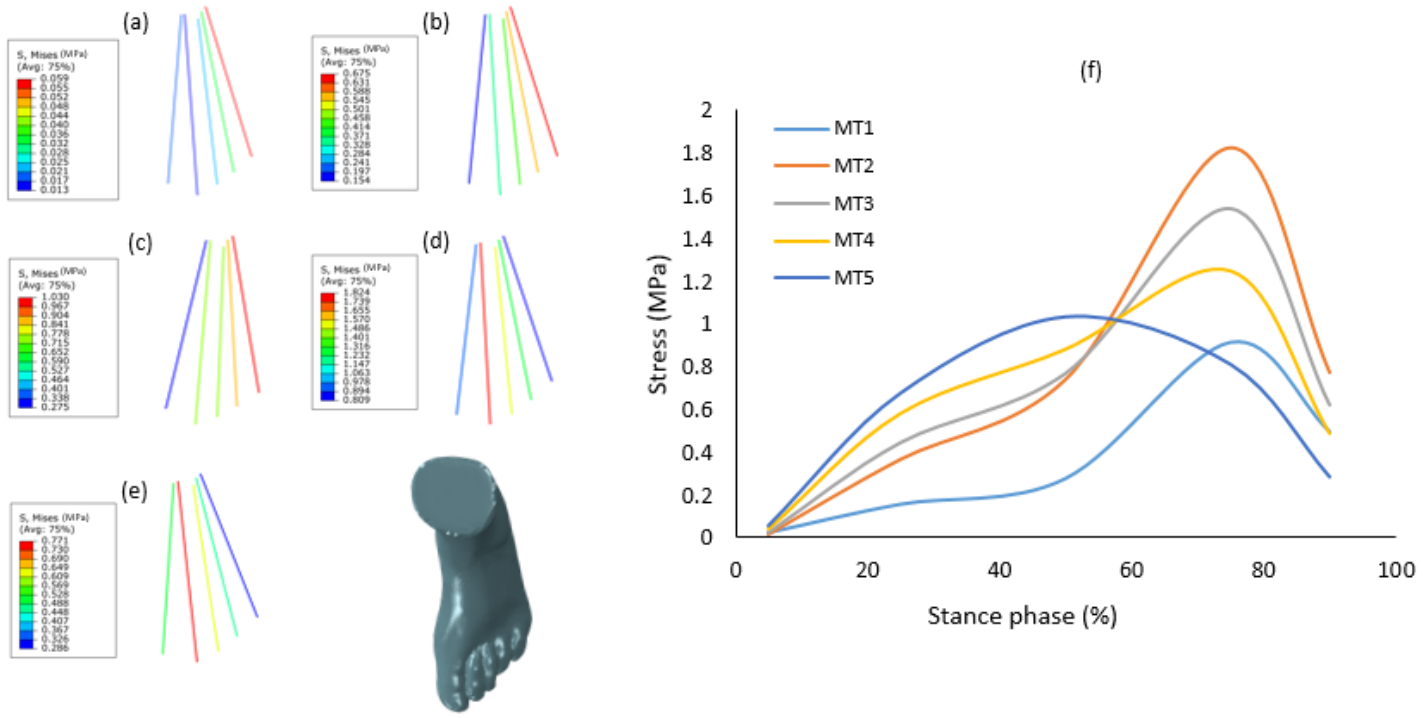

Figure 6

Plantar fascia stresses during walking at five rays of the plantar fascia in five events of stance phase at HMT foot. (a) heel strike (b) early stance (c) mid-stance (d) late stance (e) toe off (f) diagram of stress at plantar fascia rays during stance phase.

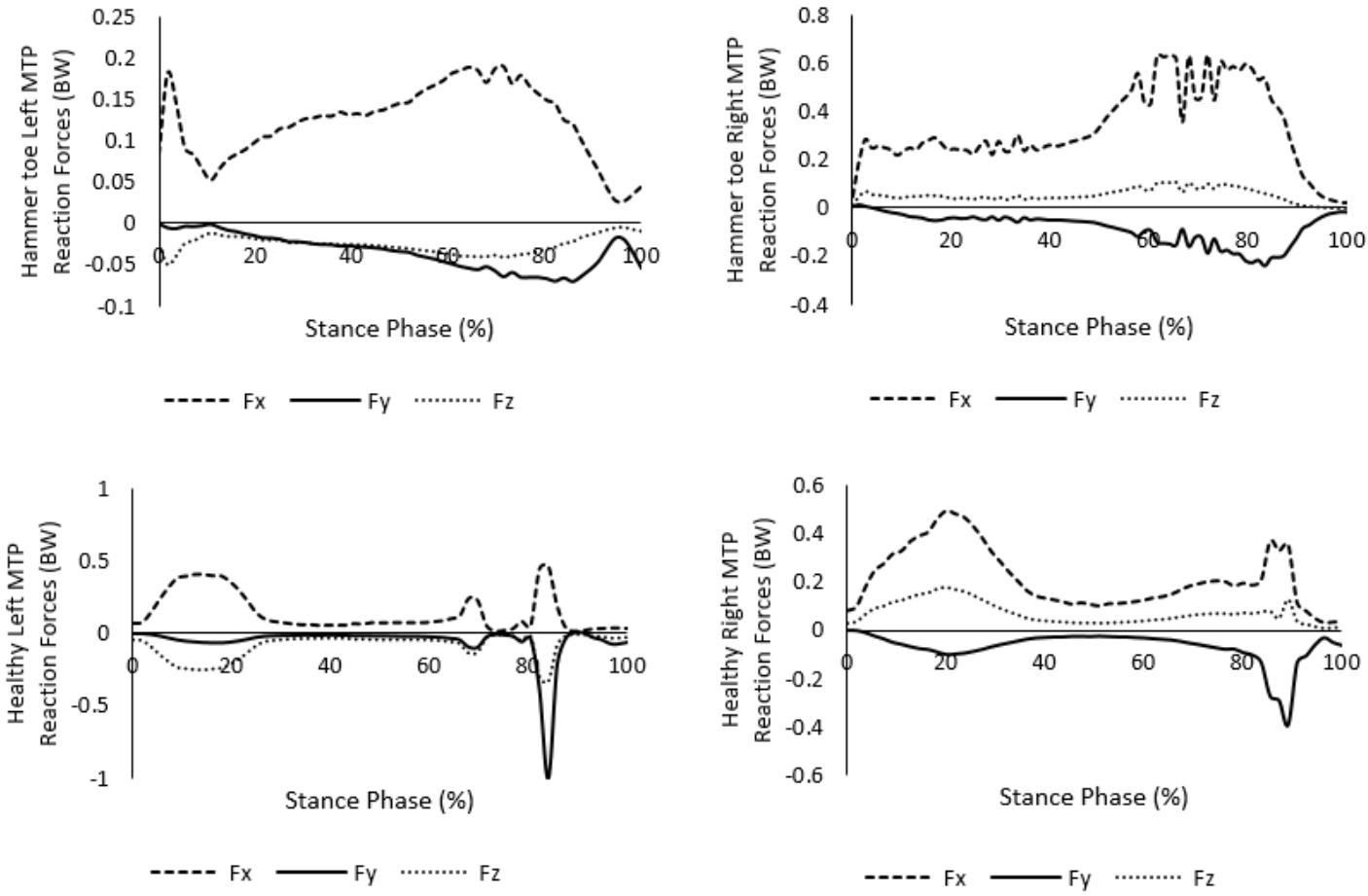

Figure 7

MTP joint reaction forces for hammer toe (left hammer toe and right healthy contralateral foot) and healthy foot participants during the stance phase normalized by body weight.

Supplementary Files

This is a list of supplementary files associated with this preprint. Click to download.

- Appendix.docx